Digital image splicing detection based on Markov features in QDCT and QWT domain

Ruxin Wang, School of Data and Computer Science, Guangdong Key Laboratory of Information Security Technology, Sun Yat-sen University, Guangzhou 510006, China

Wei Lu, School of Data and Computer Science, Guangdong Key Laboratory of Information Security Technology, Sun Yat-sen University, Guangzhou 510006, China

Shijun Xiang, College of Information Science and Technology, Jinan University, Guangzhou 510632, China.

Xianfeng Zhao, the State Key Laboratory of Information Security, Institute of Information Engineering, Chinese Academy of Sciences, Beijing 100093, China

Jinwei Wang, School of Computer and Software, Nanjing University of Information Science and Technology, Nanjing, China

ABSTRACT

Image splicing detection is of fundamental importance in digital forensics and therefore has attracted increasing attention recently. In this paper, a color image splicing detection approach is proposed based on Markov transition probability of quaternion component separation in quaternion discrete cosine transform (QDCT) domain and quaternion wavelet transform (QWT) domain. Firstly, Markov features of the intra-block and inter-block between block QDCT coefficients are obtained from the real part and three imaginary parts of QDCT coefficients respectively. Then, additional Markov features are extracted from luminance (Y) channel in quaternion wavelet transform domain to characterize the dependency of position among quaternion wavelet subband coefficients. Finally, ensemble classifier (EC) is exploited to classify the spliced and authentic color images. The experiment results demonstrate that the proposed approach can outperforms some state-of-the-art methods.

Keywords: Image splicing detection; Quaternion discrete cosine transform; Quaternion wavelet transform; Markov features; Ensemble classifier

INTRODUCTION

In recent years, with the rapid development of image editing software and processing technology, it has become easy to modify digital images without leaving any visible artifacts. The forged images can cause harmful social impact if these images are manipulated with malicious purpose. Therefore, developing some effective technique to distinguish forged image has become a major topic of research for people, and some useful schemes have been proposed recently.

At present, the categories of approaches for digital image authentication can be divided into two classes, referred to passive detection methods (Luo, Qu, Pan, & Huang, 2007; Elwin, Aditya, & Shankar, 2010; Birajdar & Mankar, 2013) and active detection methods (Vyas &

Lunagaria, 2014; Panchal & Srivastava, 2015; Stamm, Wu, & Liu, 2013). Active detection methods embed data into digital image. When verify the authenticity of images, the particular data is extracted from the suspicious image and it is compared with the original one. Compared with the active detection methods, passive detection methods can validate the authenticity of image without any prior information about the source image, which has attracted more and more attention recently.

Although any trace may not be left on the vision in tampered images, it would inevitably alter the underlying statistical characteristic of an image. Based on this idea, lots of researches which aiming at different kinds of image forgeries have been done. There are two common problems in image tampering: copy-move tamper and image splicing tamper. The primary mission of copy-move detection is to detect if there exists two or more similar regions in a single image, and to locate them if there is any. Recently, some novel methods about copy-move detection were proposed (Yang, Li, Lu, & Weng, 2017; Li, Yang, Lu, & Sun, 2016; Chen, Lu, Ni, Sun, & Huang, 2013).The primary mission of image splicing detection is to detect whether a given image is a composite one which is generated by cutting and joining two or more photographs (He, Lu, Sun, & Huang, 2012; Zhang, Lu, & Weng, 2016; Li, Ma, Xiao, Li, & Zhang, 2016). This paper mainly focus on the research of digital image splicing detection method.

Many image splicing detection methods based on Markov features have been proposed in recent years. Shi (Shi, Chen & Chen, 2007) proposed a natural image model which consists of statistical features extracted from the given test image as well as 2-D arrays produced by applying multi-size block DCT to the test image. The statistical features include moments of characteristic functions and Markov transition probabilities. And the method can achieve a detection accuracy rate of 91.87% on the DVMM dataset which introduced in (Ng & Chang, 2004). Significantly, we can observe that the accuracy of 98-D Markov features outperforms 168-D moment feature and 98-D Markov features contributes most to the effectiveness and efficiency of the whole approach. He et al. (2016) proposed an expanded Markov based scheme. The expanded Markov features generated from the transition probability matrices in DCT domain, and more features in DWT domain to characterize the three kinds of dependency among wavelet coefficients across positions, scales and orientations. SVM-RFE was utilized to handle the large number of features and then SVM was used as the classifier. The method can achieve detection accuracy of 93.55% on the DVMM dataset. Zhang et al. (2016) proposed an improved features of inter-block by considering the different frequency ranges of each block DCT coefficients in DCT domain, and additional features are extracted in Contourlet transform domain. The detection rate of 94.10% on the DVMM dataset. In (Li, Ma, Xiao, Li, & Zhang, 2016), a novel image splicing detection in QDCT domain is proposed. The method process color image pixels in a holistic manner and can achieve a detection accuracy rate of 92.38% on CASIA TIDE V2.0 dataset.

In approaches based on other models, Dong (Dong, Wang, Tan, & Shi, 2009) proposed an approach extracting statistical features from image run-length representation to capture the global inconsistency of pixel correlation and image edge statistics to detect the sharps edges introduced by splicing. And the improved method is similar to this method introduced by He (He, Sun, Lu, & Lu, 2011). In (Bahrami, Kot, & Fan, 2013; Rao, Rajagopalan, & Seetharaman, 2014; Bahrami, Kot, Li, & Li, 2015; Bahrami & Kot, 2014), some frameworks based on the inconsistency in the blur degree or depth information of an image were proposed. In (Bahrami, Kot, Li, & Li, 2015), the blur type differences of the regions were used to trace the inconsistency for the splicing localization. These methods are more suitable for blurred images.

Inspired by the promising performance of image splicing detection, a Markov of quaternion component separation (QCS) based scheme in QDCT and quaternion wavelet transform (QWT) domain is proposed for color image splicing detection in this paper.

The rest of this paper is organized as follows. Section 2 describes the proposed algorithm framework based on Markov model in detail. Section 3 shows the experiment results of the proposed method as well as the comparison with other schemes and discusses some implementation issues. Eventually, the conclusions are drawn in Section 4.

THE PROPOSED APPROACH

In this section, the whole framework of proposed approach is presented, followed by detailed description of each part.

Algorithm framework

The framework of proposed Markov features based approach is shown in Fig.1. Given a test color image, we not only extract Markov features in QDCT domain but also in QWT domain. Note that, in contrast to Li et al. (2016), the proposed method handles real part and three imaginary parts of QDCT coefficients respectively. Although the approach which take square root of sum of four parts of QDCT coefficients as block image QDCT coefficient proposed by Li et al. (2016) can reduce the feature dimension, it would eliminate some differences which is used to detect splicing tampering. And we only extract Markov features of horizontal and vertical differences arrays to reduce the dimension of Markov features. Besides, due to QWT's desirable advantages of approximate translation invariance, limited data redundancy and multi-resolution analysis, more Markov features are novel constructed in QWT domain. After all the related features are generated, Ensemble classifier is exploited to classify the authentic and spliced images.

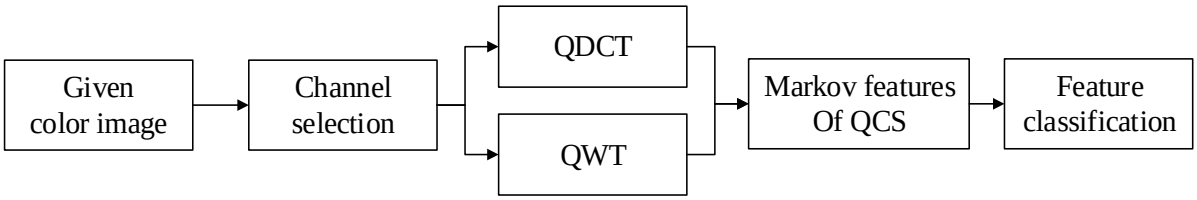

Fig. 1. Framework of the proposed algorithm

Definition and operational rule of quaternion

The famous concept of quaternions was introduced by Hamilton in Dublin in 1843. A quaternion includes four components (one real part and three imaginary part). Definition and some basic operation properties of quaternion are introduced as follows:

The definition of quaternion

$$q = a + b \cdot i + c \cdot j + d \cdot k \tag{1}$$

Where $a, b, c, d \in R$ and i, j, k obey the following Hamilton rule

$$\begin{aligned} &i^2 = j^2 = k^2 = -1 \\ &i \cdot j = -j \cdot i = k, k \cdot i = -i \cdot k = j \\ &j \cdot k = -k \cdot j = i \end{aligned} \tag{2}$$

which demonstrates that the multiplication of quaternions is not commutative. The conjugate of quaternion is $\bar{q} = a - b \cdot i - c \cdot j - d \cdot k$, and the modulus of a quaternion q follows the definition of complex numbers

$$|q|=\sqrt{a^2+b^2+c^2+d^2} \tag{3}$$

MARKOV FEATURES OF QCS IN QDCT DOMAIN

Quaternion discrete cosine transform

The basic principle of quaternion discrete cosine transform was proposed by Feng and Hu (Feng & Hu, 2008). Due to the non-commutative multiplication rule of quaternions, QDCT has left-handed form and right-handed form, which satisfy the following equations, respectively:

$$F_q^L(p,s)=\alpha(p)\alpha(s)\sum_{m=0}^{M-1}\sum_{n=0}^{N-1}u_q\cdot f_q(m,n)\cdot N(p,s,m,n) \tag{4}$$

$$F_q^R(p,s)=\alpha(p)\alpha(s)\sum_{m=0}^{M-1}\sum_{n=0}^{N-1}f_q(m,n)\cdot N(p,s,m,n)\cdot u_q \tag{5}$$

where u_q is a unit pure quaternion which satisfies $u_q^2=-1$, $f(m,n)$ is a two-dimensional $M\times N$ quaternion matrix. Similar to DCT in real number and complex number domain the definition of $a(p),a(s)$ are as follows:

$$\alpha(p)=\begin{cases}\sqrt{\dfrac{1}{M}}, p=0\\ \sqrt{\dfrac{2}{M}}, p\neq 0\end{cases} \tag{6}$$

$$\alpha(s)=\begin{cases}\sqrt{\dfrac{1}{N}}, s=0\\ \sqrt{\dfrac{2}{N}}, s\neq 0\end{cases} \tag{7}$$

$$N(p,s,m,n)=\cos\left[\frac{\pi(2m+1)p}{2M}\right]\cos\left[\frac{\pi(2n+1)s}{2N}\right] \tag{8}$$

The spectral coefficient of $F(p,s)$ through transformation is still a quaternion matrix, and it can be presented as follow:

$$F(p,s)=F_0(p,s)+F_1(p,s)\cdot i+F_2(p,s)\cdot j+F_3(p,s)\cdot k \tag{9}$$

Block QDCT

In this paper, we chose Left-QDCT and the Clay-Dickson theorem (Moxey, Sangwine, & Ell, 2003) to perform QDCT transform. The first and second steps of block QDCT are the same as steps in Part 3.3 (Li, Ma, Xiao, Li, & Zhang, 2016). Firstly, the original color images are blocked into 8×8 non-repeatedly, and three color components of R, G and B of blocked image are utilized to construct quaternion matrix. Secondly, Left-QDCT is used to obtain QDCT coefficient matrix of each block. Finally, we extract real part and three imaginary parts of calculated matrix respectively to reassemble according to the site of blocking, thus four 8×8 blocked QDCT component coefficient matrices can be obtained which including real matrix (F_0) and three imaginary matrices (F_1,F_2,F_3).

Extraction of features

We only extract Markov features of horizontal and vertical differences arrays between intra-block and inter-block in QDCT domain by considering dimension of features. The following steps are shown.

Firstly, apply 8×8 block QDCT on the original image pixel array and four corresponding QDCT component coefficient arrays F_0, F_1, F_2, F_3 are obtained. Because all the next steps of four component coefficients matrices will use the same methods, we use real matrix (F_0) for an example.

Secondly, round the coefficients in F_0 to integer and take absolute value (denote the obtained arrays F).

Thirdly, intra-block difference arrays are calculated along the horizontal and vertical directions by applying Eqs. (10) to (11), denoted by D_h and D_v respectively.

$$D_h = F(u,v) - F(u+1,v) \tag{10}$$

$$D_v = F(u,v) - F(u,v+1) \tag{11}$$

And inter-block difference arrays are calculated along the horizontal and vertical directions by applying Eqs. (12) to (13), denoted by G_h and G_v respectively.

$$G_h = F(u,v) - F(u+8,v) \tag{12}$$

$$G_v = F(u,v) - F(u,v+8) \tag{13}$$

where u and v denote coordinates in corresponding matrix. Then a truncation value T ($T \in N^+$) is introduced to reduce the computational complexity and to limit the risk of overfitting. If an element of D_h(D_v, G_h, G_v) is either larger than T or smaller than $-T$, it will be represented by T or $-T$ correspondingly.

Fourthly, the intra-block and inter-block transition probability matrices used to characterize Markov process are constructed along the horizontal and vertical directions on the above four difference arrays, denoted by D_{hh}, D_{hv}, D_{vh}, D_{vv}, G_{hh}, G_{hv}, G_{vh} and G_{vv}.

$$D_{hh}(i,j) = \frac{\sum_{u=1}^{S_u-2}\sum_{v=1}^{S_v}\delta(D_h(u,v)=i, D_h(u+1,v)=j)}{\sum_{u=1}^{S_u-2}\sum_{v=1}^{S_v}\delta(D_h(u,v)=i)} \tag{14}$$

$$D_{hv}(i,j) = \frac{\sum_{u=1}^{S_u-1}\sum_{v=1}^{S_v-1}\delta(D_h(u,v)=i, D_h(u,v+1)=j)}{\sum_{u=1}^{S_u-1}\sum_{v=1}^{S_v-1}\delta(D_h(u,v)=i)} \tag{15}$$

$$D_{vh}(i,j) = \frac{\sum_{u=1}^{S_u-1}\sum_{v=1}^{S_v-1}\delta(D_h(u,v)=i, D_h(u+1,v)=j)}{\sum_{u=1}^{S_u-1}\sum_{v=1}^{S_v-1}\delta(D_v(u,v)=i)} \tag{16}$$

$$D_{vv}(i,j) = \frac{\sum_{u=1}^{S_u}\sum_{v=1}^{S_v-2}\delta(D_h(u,v)=i, D_h(u,v+1)=j)}{\sum_{u=1}^{S_u}\sum_{v=1}^{S_v-2}\delta(D_v(u,v)=i)} \tag{17}$$

$$G_{hh}(i,j) = \frac{\sum_{u=1}^{S_u-16}\sum_{v=1}^{S_v}\delta(G_h(u,v)=i, G_h(u+8,v)=j)}{\sum_{u=1}^{S_u-16}\sum_{v=1}^{S_v}\delta(G_h(u,v)=i)} \tag{18}$$

$$G_{hv}(i,j)=\frac{\sum_{u=1}^{S_u-8}\sum_{v=1}^{S_v-8}\delta(G_h(u,v)=i,G_h(u,v+8)=j)}{\sum_{u=1}^{S_u-8}\sum_{v=1}^{S_v-8}\delta(G_h(u,v)=i)} \tag{19}$$

$$G_{vh}(i,j)=\frac{\sum_{u=1}^{S_u-8}\sum_{v=1}^{S_v-8}\delta(G_h(u,v)=i,G_h(u+8,v)=j)}{\sum_{u=1}^{S_u-8}\sum_{v=1}^{S_v-8}\delta(G_v(u,v)=i)} \tag{20}$$

$$G_{vv}(i,j)=\frac{\sum_{u=1}^{S_u}\sum_{v=1}^{S_v-16}\delta(G_h(u,v)=i,G_h(u,v+8)=j)}{\sum_{u=1}^{S_u}\sum_{v=1}^{S_v-16}\delta(G_v(u,v)=i)} \tag{21}$$

where $i,j\in\{-T,-T+1,...,-1,0,1,...,T-1,T\}$, S_u and S_v denote the dimensions of the original source image. $\delta(\cdot)=1$ only when its arguments are satisfied, otherwise $\delta(\cdot)=0$ .Thus $(2T+1)\times(2T+1)\times 8\times 4$ dimensionality Markov features in QDCT domain are totally obtained.

MARKOV FEATURES OF QCS IN QWT DOMAIN

"The quaternion wavelet transform (QWT) is first proposed in 2004, as a natural extension of real and complex wavelet." (Shen, Feng, Wang, Liu, & He, 2014). QWT has the advantages of approximate translation invariance, rich phase information, limited data redundancy while preserving the good localized time-frequency localization capability of traditional wavelet. Many researches about theory and application of QWT have been proposed in the past, such as (Bayro-Corrochano, 2006; Shen, Feng, Wang, Liu, & He, 2014; Wang, Lin, Shi, Lian, & Ye, 2016). In (Bayro-Corrochano, 2006), the major contribution of this paper is that it generalizes the real and complex wavelet transforms and derives a quaternionic wavelet pyramid for multi-resolution analysis using the quaternionic phase concept. Shen et al. (2014) proposed to combine the standard support vector machine (SVM) classification technique with the quaternion wavelet transform (QWT) to enhance the classification accuracy of hyperspectral image. In (Wang, Lin, Shi, Lian, & Ye, 2016), a novel method based on QWT is proposed for distinguishing photographic (PG) images and computer generated (CG) images. To sum up, QWT is a useful tool for image processing.

Due to QWT's advantages, we introduced QWT to detect splicing image in this paper. If an image is decomposed by quaternion wavelet, we can obtain four subbands: approximation subband, horizontal detail subband, vertical detail subband and diagonal subband. And each subband coefficient is also quaternion. As shown in Fig.3, we can obtain 7 subbands through two-level quaternion wavelet decomposition, and we can obtain 28 matrices when we extract real part and three imaginary parts of each subband coefficient respectively to reassemble component coefficients matrices.

In this paper, the filter in quaternion wavelet decomposition is a double tree filter bank. The first layer filter uses an approximately symmetric orthogonal Farrs band (Abdelnour & Selesnick, 2001), and Q-Shift double tree filter is used from second layer (Kingsbury, 2001). Here, we resort to Markov random process (Transition Probability Matrix) to capture the dependency among quaternion wavelet subband coefficients across position for image splicing detection. And the Markov features in QWT domain can be calculated as follows.

Firstly, two-level quaternion wavelet transform is applied to decompose the luminance (Y) channel of the given color image. Then 28 component matrices of subband coefficients can be obtained. We round all the coefficients of 28 component matrices to integer and take absolute value. Let C_k denote the k component matrix and k denote the total number of the obtained matrices, so $k\in\{1,2,...,28\}$.

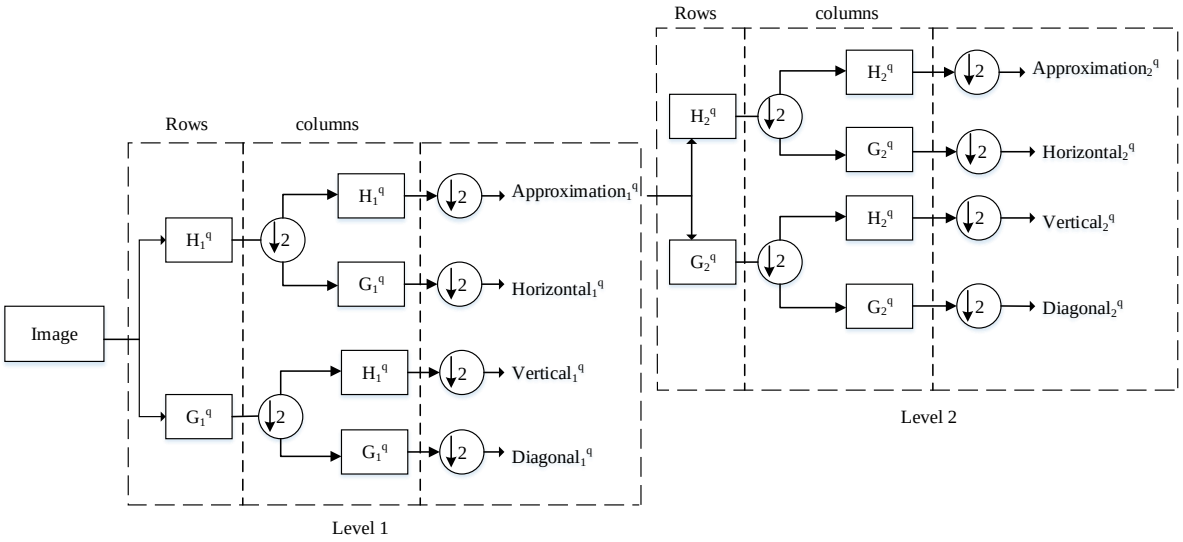

Fig. 2. Structure of two-level quaternion wavelet decomposition

Secondly, steps similar to use Markov transition probability matrices to characterize the correlation of neighboring DCT coefficients in the intra-block are used to represent the dependency of positions among coefficients. Then the horizontal and vertical difference arrays of k component matrix denoted by D_{kh} and D_{kv} are calculated as follows.

$$D_{kh}(u,v) = C_k(u,v) - C_k(u+1,v) \tag{22}$$

$$D_{kv}(u,v) = C_k(u,v) - C_k(u,v+1) \tag{23}$$

where u and v denote coordinates in corresponding matrix. Then a truncation value T ($T \in N^+$) is introduced to reduce the computational complexity and to limit the risk of overfitting. If an element of D_{kh} or D_{kv} is either larger than T or smaller than $-T$, it will be represented by T or $-T$ correspondingly.

Thirdly, the transition probability matrices used to characterize Markov process are constructed along the horizontal and vertical directions on the above two difference arrays, denoted by D_{khh}, D_{khv}, D_{kvh}, D_{kvv}.

$$D_{khh}(i,j) = \frac{\sum_{u=1}^{S_{ku}-2}\sum_{v=1}^{S_{kv}}\delta(D_{kh}(u,v)=i, D_{kh}=(u+1,v)=j)}{\sum_{u=1}^{S_{ku}-2}\sum_{v=1}^{S_{kv}}\delta(D_{kh}(u,v)=i)} \tag{24}$$

$$D_{khv}(i,j) = \frac{\sum_{u=1}^{S_{ku}-1}\sum_{v=1}^{S_{kv}-1}\delta(D_{kh}(u,v)=i, D_{kh}=(u,v+1)=j)}{\sum_{u=1}^{S_{ku}-1}\sum_{v=1}^{S_{kv}-1}\delta(D_{kh}(u,v)=i)} \tag{25}$$

$$D_{kvh}(i,j) = \frac{\sum_{u=1}^{S_{ku}-1}\sum_{v=1}^{S_{kv}-1}\delta(D_{kv}(u,v)=i, D_{kv}=(u+1,v)=j)}{\sum_{u=1}^{S_{ku}-1}\sum_{v=1}^{S_{kv}-1}\delta(D_{kv}(u,v)=i)} \tag{26}$$

$$D_{kvv}(i,j) = \frac{\sum_{u=1}^{S_{ku}}\sum_{v=1}^{S_{kv}-2}\delta(D_{kv}(u,v)=i, D_{kv}=(u,v+1)=j)}{\sum_{u=1}^{S_{ku}}\sum_{v=1}^{S_{kv}-2}\delta(D_{kv}(u,v)=i)} \tag{27}$$

where $i, j \in \{-T, -T+1, ..., -1, 0, 1, ..., T-1, T\}$, S_{ku} and S_{kv} denote the dimensions of the original source image. $\delta(\cdot)=1$ only when its arguments are satisfied, otherwise $\delta(\cdot)=0$. Thus $(2T+1)\times(2T+1)\times 4\times 28$ dimensionality Markov features in QWT domain are totally obtained.

FEATURE CLASSIFICATION

In total, $(2T+1)\times(2T+1)\times 144$ dimensionality Markov features of QCS in QDCT and QWT domain are obtained from given color image. The classification method SVM is unsuitable because the dimensionality of the final features is too large and the computation complexity is too high.

Ensemble classifier which implemented on random forests is a scalable machine learning tool (Kodovský, Fridrich, & Holub, 2012; Kodovský & Fridrich, 2011). And it consists of many base learners independently trained on a set of subspace of the feature space. The final decision of a given color image is formed by aggregating the decisions of all individual base learners. Although the performance of individual base learners may be weak, the accuracy of classification will improve quickly after composite. To further improve the mutual diversity of the base learners, every base learner is trained on a bootstrap sample which uniformly and randomly selected from the whole training set. Ensemble classifier can substantially speed up the development cycle while allowing the classification to work with very complex and potentially high dimensional feature vectors as well as large training sets. More details about ensemble classifier can be found (Kodovský, Fridrich, & Holub, 2012; Kodovský & Fridrich, 2011). So, we chose ensemble classifier to classify the authentic and spliced color images in this paper.

EXPERIMENTS AND DISCUSSIONS

In this section, we first introduce the image datasets used in experiment and some details about experiment parameters, and then present a set of experiments to demonstrate the effectiveness of the proposed features in different domain. Finally, we make a comparison with other image splicing detection approaches which joint two kinds domain to demonstrate effectiveness and high performance of the proposed method.

Experiment conditions

To evaluate the effectiveness of the proposed Markov features extracted in QWT domains, some experiments are conducted over the DVMM dataset (Ng & Chang, 2004). The public available DVMM dataset were provided by the DVMM Laboratory of Columbia University for benchmarking the blind passive image splicing detection algorithms. It consists of 933 authentic and 912 spliced images with a fixed size of 128×128 pixels. And all image blocks come from gray images. More details about the DVMM dataset may be found in (Ng & Chang, 2004). Some example images of the dataset are shown in Fig. 3 where the authentic images are given in the first row and the spliced images are given in the second row.

In order to demonstrate the effectiveness of the proposed Markov features extracted in QDCT domains and the detection performance of the proposed approach, some experiments are conducted over IEEE Information Forensics and Security Technical Committee (IFS-TC) dataset which is introduced in (Cozzolino, Gragnaniello, & Verdoliva, 2014; Verdoliva, Cozzolino, & Poggi, 2014). The original images of ITF-TC dataset captured from different digital cameras with various scenes either indoor or outdoor. The forged images comprise a set of different manipulation techniques such as copy/pasting and splicing with different degrees of photorealism. Some example images of the dataset are shown in Fig. 4 where the authentic images are given in the first row and the spliced images are given in the second row.

There also have three public image datasets for color image splicing detection including color image dataset of DVMM, CASIA TIDE V1.0 and CASIA TIDE V2.0. The color image

dataset of DVMM only contain 183 authentic color images and 180 spliced color images, the amount of data of color images dataset is few. There are two problems of the dataset CASAI TIDE V1.0 and CASAI TIDE V2.0 have been pointed out by Sutthiwan (Sutthiwan, Shi, Zhao, Ng, & Su). First one is the JPEG compression applied to authentic images is one-time less than that applied to tampered images; the second one is for JPEG images, the size of chrominance components of 7,140 authentic images is only one quarter of that of 2,061 tampered images. So, we do not conduct experiment on these three color image datasets. In order to better verify our proposed approach, we chose gray image dataset of DVMM and IFS-TC dataset which introduced above.

In experiments, image splicing detection is consider as a binary decision problem, authentic images are labeled as +1 while spliced images are labeled as -1. We set $T = 4$ for splicing detection with manageable computational complexity. In order to compare the effectiveness of features extracted in QDCT domain and QWT domain respectively with other similar methods in a fair environment, we chose LIBSVM (Chang & Lin, 2010) which used in other methods to classify the authentic images and spliced images. And we chose ensemble classifier to better demonstrate the detection performance of the whole approach with high dimension feature.

In the classification phase of each experiment, 20 random training and testing are performed independently to reduce the variations caused by different selections of the training samples and the testing samples. In each of the 20 runs, 5/6 of authentic images and 5/6 of spliced images in the dataset are randomly selected to train the corresponding classifier, then the remaining 1/6 of the authentic and spliced images are used to test the trained classifier. We measure the detection performance by the following criterions: TP (true positive) rate, TN (true negative) rate, accuracy and the AUC. TP rate is the ratio of correct classification of authentic images while TN rate is the ratio of correct classification of spliced images. Accuracy can be obtained by averaging the weighted value of TP rate and TN rate. And the AUC is the value of the area under ROC curve. The testing platform is Matlab R2015a, and hardware platform is a PC with 8G core i5 processor.

Fig. 3. Some samples of DVMM dataset. Row one to row two show authentic image and spliced images

Fig. 4. Some samples of IFS-TC dataset. Row one to row two show authentic image and spliced images

Effectiveness of different parts

We will evaluate the effectiveness of the proposed Markov features extracted in QDCT domains on IFS-TC dataset and evaluate the effectiveness of the proposed Markov features extracted in QWT domains on DVMM dataset.

Firstly, the experiments on the IFS-TC dataset with the features in QDCT domain are implemented to examine the contributions made by the Markov features of QCS in the proposed approach. The detailed results are given in Table 1, we reduced the dimensionality of features similar to Li et al. (2016) to make the computational complexity manageable.

And to better evaluate the effectiveness of the proposed Markov features extracted in QDCT domains, some comparative experiments between the proposed methods and some similar methods in (He, Lu, Sun, & Huang, 2012; Zhang, Lu, & Weng, 2016; Li, Ma, Xiao, Li, & Zhang, 2016) are implemented on IFS-TC dataset. The detailed results are given in Table 2 and the corresponding ROC curves are shown in Fig. 5. The dimensionality of corresponding features before feature selection are given in the bracket in Table 1 and Table 2.

As shown in Table 2 and Fig.5, it can be observed that the detection performance of the features of QCS in QDCT domain is better than other similar methods. It may be because features proposed in this paper are more fully exploited the relevance of color information.

Table 1

Experiment results of QDCT features with different threshold T on IFS-TC training set

Threshold *T*	Dimensionality *n*	TP (%)	TN (%)	Accuracy (%)
3	588 (1568)	91.71	90.67	**91.14**
4	972 (2592)	94.89	87.50	**92.30**
5	1452 (3872)	93.33	92.24	**92.73**

Table 2
Comparison on the detection results of QDCT or DCT between the proposed approach and other similar methods on the IFS-TC training set (T =4)

Methods	DCT(He, Lu, Sun, & Huang, 2012)	DCT(Zhang, Lu, & Weng, 2016)	QDCT(Li, Ma, Xiao, Li, & Zhang, 2016)	QDCT (Proposed)
Dimensionality	648	972 (3888)	972	972 (2592)
TP (%)	86.07	88.43	91.38	94.89
TN (%)	83.96	90.54	88.14	87.50
Accuracy (%)	85.11	89.58	89.61	**92.30**

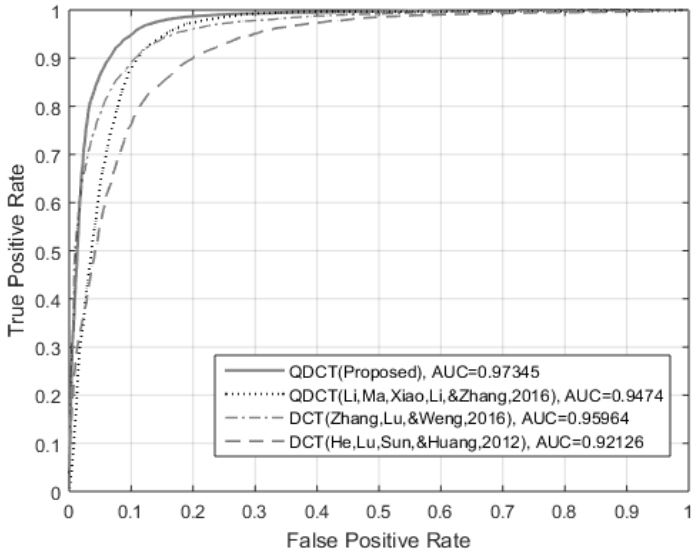

Fig. 5. The ROC curves of different feature vectors on the IFS-TC training set

Secondly, the experiments on the DVMM dataset with Markov features of two-level QWT subband coefficients are implemented to examine the contributions made by the Markov features of QWT domain. In our experiments, Markov features are extracted from L_1, L_2 and dimensionality of feature is set to 50, 100, 150 or 200 to verify the effectiveness of features as well as make the computational complexity manageable. The detailed results are given Table 3. To better evaluate the effectiveness of the proposed Markov features extracted in QWT domains, some comparative experiments between the proposed methods and other methods in (He, Lu, Sun, & Huang, 2012; Zhang, Lu, & Weng, 2016) are implemented on DVMM dataset. The detailed results are given in Table 4 and the corresponding ROC curves are shown in Fig. 6. The dimensionality of corresponding features before feature selection are given in the bracket in Table 4.

As shown in Table 3, with the increase of dimensionality, the features of two-level QWT can achieve a detection accuracy as high as 86.91%, it may be because the features with high dimension in QWT domain are more effective to reveal the difference between authentic and spliced images. And it can be easily noticed from the experiment results that the features of

QWT outperforms the features in DWT domain and Contourlet domain on the DVMM dataset in Table 4 and Fig .6.

Table 3

Detection results of different dimensionality of features in QWT domain on the DVMM dataset (T =4)

Dimensionality *n*	TP (%)	TN (%)	Accuracy (%)
50	84.34	84.37	**84.35**
100	86.15	85.75	**85.95**
150	86.49	85.88	**86.19**
200	86.90	86.92	**86.91**

Table 4

Comparison on the detection results of QWT, Contourlet and DWT between the proposed approach and other methods on the DVMM dataset (T =4)

Methods	DWT (He, Lu, Sun,& Huang, 2012)	Contourlet (Zhang,Lu, & Weng, 2016)	QWT (Proposed)
Dimensionality *n*	200 (4212)	200 (4212)	200 (9072)
TP (%)	86.43	81.99	86.90
TN (%)	83.21	82.92	86.92
Accuracy (%)	84.83	82.45	**86.91**

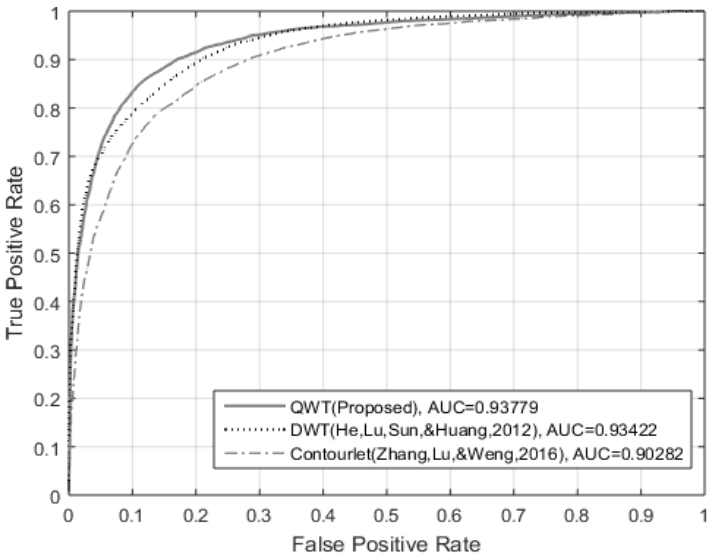

Fig. 6. The ROC curves of different feature vectors on the DVMM set

Detection performance of the proposed approach

To evaluate the proposed whole approach comprehensively, some common experiments are conducted on the IFS-TC dataset. As mentioned above, the threshold T is set to 3, 4, 5 respectively. Then ensemble classifier is exploited to classification for these features. The details are presented in Table 5. As shown in Table 5, it can be observed that when T =5, the proposed approach performs better than when T =3 or T =4, as is expected. However, we can also see that, compared with setting T = 5, setting T =4 does not cause a dramatic drop in detection rates. Thus, to make the computational complexity manageable, a threshold T =4 might be more suitable.

We also make some comparative experiments between the proposed approach and some other methods which joint two kinds domain, such as He et al. (2012) and Zhang et al. (2016). In He et al. (2012), the Markov features are not only extracted from coefficients of intra-block and inter-block in DCT domain but also extracted from wavelet coefficients across positions, scales and orientations in DWT domain. Zhang et al. (2016) improved the inter-block Markov features by considering the different frequency ranges of block DCT coefficients, and also extracted Markov features from Contourlet domain.

For these methods, we chose to compare with their best detection performance on the IFS-TC training set. So SVM-RFE and SVM is used for He et al. (2012), and ensemble classifier is used for Zhang et al. (2016) and the proposed approach. The detailed results of comparisons and corresponding ROC curves of each method are given in Table 6 and Fig. 7. As shown in Table 6 and Fig .7, the proposed approach outperforms the other approaches introduced in our experiment. It can also be noticed that the dimensionality of our features is less than Zhang and the detection accuracy of the proposed approach is higher than Zhang, which demonstrates that the proposed approach is suitable for digital image splicing detection.

To sum up, the experiment results show that the proposed approach can achieve an excellent detection performance on the IFS-TC training set, and demonstrate the effectiveness of the proposed approach for color image splicing detection. What is more, the proposed approach improves the detection accuracy on the IFS-TC training set in comparison to other Markov based approaches introduced in (He, Lu, Sun, & Huang, 2012; Zhang, Lu, & Weng, 2016; Li, Ma, Xiao, Li, & Zhang, 2016).

Table 5

Experiment results of proposed method with different threshold T on the IFS-TC training set

Threshold *T*	Dimensionality *n*	TP (%)	TN (%)	Accuracy (%)
3	7056	95.63	91.25	**93.44**
4	11664	96.75	95.13	**95.94**
5	17424	97.50	95.00	**96.25**

Table 6
Comparison on the detection results between the proposed approach and other methods on the IFS-TC training set (T =4)

Methods	He, Lu, Sun, & Huang, 2012	Zhang, Lu, & Weng, 2016	Proposed
Dimensionality *n*	100 (7290)	16524	11664
TP (%)	96.01	96.25	**96.75**
TN (%)	90.54	93.75	**95.13**
Accuracy (%)	93.03	95.00	**95.94**

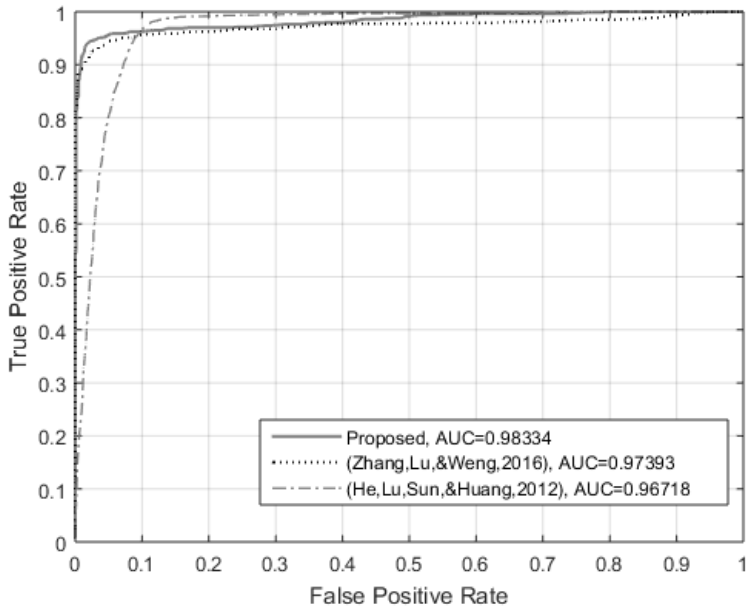

Fig. 7. The ROC curves of different methods on the IFS-TC training set

CONCLUSION

In this paper, a color image splicing detection approach based on Markov of quaternion component separation in QDCT domain and QWT domain is proposed. In QDCT domain, we extract intra-block and inter-block Markov features from real part and the three imaginary parts of QDCT coefficients respectively. Additional features are extracted from luminance (Y) channel in quaternion wavelet transform domain to characterize the dependency of position among quaternion wavelet subband coefficients. In order to handle the large number of obtained features, ensemble classifier is exploited to classify the authentic and spliced color image. Experiment results demonstrates that the proposed approach has a desirable generalization ability for color image splicing detection.

ACKNOWLEDGEMENTS

This work is supported by the Natural Science Foundation of Guangdong (No. 2016A030313350), the Special Funds for Science and Technology Development of Guangdong (No. 2016KZ010103), the Fundamental Research Funds for the Central Universities (No. 16lgjc83 and No. 17lgjc45), and Scientific and Technological Achievements Transformation Plan of Sun Yat-sen University.

REFERENCE

Abdelnour, A. F., & Selesnick, I. W. (2001, May). Nearly symmetric orthogonal wavelet bases. *Proceedings of the IEEE International Conference on Acoustics, Speech and Signal Processing (ICASSP).*

Bahrami, K., & Kot, A. C. (2014, May). Image tampering detection by exposing blur type inconsistency. *Proceedings of the IEEE International Conference on Acoustics, Speech and Signal Processing (ICASSP) (pp. 2654-2658).*

Bahrami, K., Kot, A. C., Li, L., & Li, H. (2015). Blurred image splicing localization by exposing blur type inconsistency. *IEEE Transactions on Information Forensics and Security*, 10(5), 999-1009.

Bahrami, K., Kot, A. C., & Fan, J. (2013, November). Splicing detection in out-of-focus blurred images. *Proceedings of the IEEE International Workshop on Information Forensics and Security (WIFS) (pp. 144-149).*

Bayro-Corrochano, E. (2006). The theory and use of the quaternion wavelet transform. *Journal of Mathematical Imaging and Vision*, 24(1), 19-35.

Birajdar, G. K., & Mankar, V. H. (2013). Digital image forgery detection using passive techniques: A survey. *Digital Investigation*, 10(3), 226-245.

C.-C. Chang, C.-J. Lin, (2010) LIBSVM – a library for support vector machines, from http://www.csie.ntu.edu.tw/cjlin/libsvm

Chen, L., Lu, W., Ni, J., Sun, W., & Huang, J. (2013). Region duplication detection based on Harris corner points and step sector statistics. *Journal of Visual Communication and Image Representation*, 24(3), 244-254.

Cozzolino, D., Gragnaniello, D., & Verdoliva, L. (2014, October). Image forgery localization through the fusion of camera-based, feature-based and pixel-based techniques. *Proceedings of the IEEE International Conference on Image Processing (ICIP) (pp. 5302-5306).*

Dong, J., Wang, W., Tan, T., & Shi, Y. Q. (2008, November). Run-Length and Edge Statistics Based Approach for Image Splicing Detection. *Proceedings of 7th International Workshop on Digital Watermarking (IWDW) (pp. 76-87).*

Elwin, J. G. R., Aditya, T. S., & Shankar, S. M. (2010, December). Survey on passive methods of image tampering detection. *Proceedings of International Conference on Communication and computational intelligence (INCOCCI) (pp. 431-436).*

Feng, W., & Hu, B. (2008, May). Quaternion discrete cosine transform and its application in color template matching. *Proceedings of the Congress on Image and Signal Processing (Vol. 2, pp. 252-256).*

He, Z., Lu, W., Sun, W., & Huang, J. (2012). Digital image splicing detection based on Markov features in DCT and DWT domain. *Pattern Recognition*, 45(12), 4292-4299.

He, Z., Sun, W., Lu, W., & Lu, H. (2011). Digital image splicing detection based on approximate run length. *Pattern Recognition Letters*, 32(12), 1591-1597.

Kingsbury, N. (2001). Complex wavelets for shift invariant analysis and filtering of signals. *Applied and computational harmonic analysis*, 10(3), 234-253.

Kodovský, J., & Fridrich, J. J. (2011, January). Steganalysis in high dimensions: fusing classifiers built on random subspaces. *In Media Watermarking, Security, and Forensics III* (181-197). California, USA, SPIE.

Kodovský, J.., Fridrich, J., & Holub, V. (2012). Ensemble classifiers for steganalysis of digital media. *IEEE Transactions on Information Forensics and Security*, 7(2), 432-444.

Li, C., Ma, Q., Xiao, L., Li, M., & Zhang, A. (2017). Image splicing detection based on Markov features in QDCT domain. *Neurocomputing*, 228, 29-36.

Li, J., Yang, F., Lu, W., & Sun, W. (2016). Keypoint-based copy-move detection scheme by adopting MSCRs and improved feature matching. *Multimedia Tools and Applications*, 1-15.

Luo, W., Qu, Z., Pan, F., & Huang, J. (2007). A survey of passive technology for digital image forensics. *Frontiers of Computer Science in China*, 1(2), 166-179.

Moxey, C. E., Sangwine, S. J., & Ell, T. A. (2003). Hypercomplex correlation techniques for vector images. *IEEE Transactions on Signal Processing*, 51(7), 1941-1953.

Ng, T. T., Chang, S. F., & Sun, Q. (2004). A data set of authentic and spliced image blocks. *Columbia University, ADVENT Technical Report*, 203-2004.

Panchal, U. H., & Srivastava, R. (2015, April). A comprehensive survey on digital image watermarking techniques. *Proceedings of the Fifth International Conference on Communication Systems and Network Technologies (CSNT) (pp. 591-595).*

Rao, M. P., Rajagopalan, A. N., & Seetharaman, G. (2014). Harnessing motion blur to unveil splicing. *IEEE Transactions on Information Forensics and Security*, 9(4), 583-595.

Shen, Y., Feng, H., Wang, Q., Liu, Y., & He, Z. (2014, May). QWT enhanced SVM for Hyperspectral image classification. *Proceedings of the IEEE International Instrumentation and Measurement Technology Conference (I2MTC) (pp. 1454-1458).*

Shi, Y. Q., Chen, C., & Chen, W. (2007, September). A natural image model approach to splicing detection. *Proceedings of the 9th ACM workshop on Multimedia & security (pp. 51-62)*

Stamm, M. C., Wu, M., & Liu, K. R. (2013). Information forensics: An overview of the first decade. *IEEE Access*, 1, 167-200.

Sutthiwan, P., Shi, Y. Q., Zhao, H., Ng, T. T., & Su, W. (2011). Markovian rake transform for digital image tampering detection. *In Transactions on data hiding and multimedia security VI* (pp. 1-17). Berlin, Heidelberg, Springer.

Verdoliva, L., Cozzolino, D., & Poggi, G. (2014, December). A feature-based approach for image tampering detection and localization. *Proceedings of the IEEE International Workshop on Information Forensics and Security (WIFS) (pp. 149-154).*

Vyas, C., & Lunagaria, M. (2014, December). A review on methods for image authentication and visual cryptography in digital image watermarking. *Proceedings of the IEEE International Conference on Computational Intelligence and Computing Research (ICCIC)* (pp. 1-6).

Wang, J., Li, T., Shi, Y. Q., Lian, S., & Ye, J. (2016). Forensics feature analysis in quaternion wavelet domain for distinguishing photographic images and computer graphics. *Multimedia Tools & Applications*, 1-17.

Yang, F., Li, J., Lu, W., & Weng, J. (2017). Copy-move forgery detection based on hybrid features. *Engineering Applications of Artificial Intelligence*, 59, 73-83.

Zhang, Q., Lu, W., & Weng, J. (2016). Joint image splicing detection in DCT and Contourlet transform domain. *Journal of Visual Communication and Image Representation*, 40, 449-45